RSC Advances

PAPER

View Article Online
View Journal | View Issue

Cite this: *RSC Adv.*, 2022, **12**, 22060

Adsorptive separation of *para*-xylene by nonporous adaptive crystals of phenanthrene[2]arene†

Ying Hou, Yin-Rong Duan, Man-Hua Ding,* Lin-Li Tang and Fei Zeng *

Received 19th June 2022
Accepted 3rd August 2022

DOI: 10.1039/d2ra03773d

rsc.li/rsc-advances

In this work, we developed a new method for the preparation of phenanthrene[2]arene on a large-scale. Meanwhile, the synthetic phenanthrene[2]arene has been successfully used as nonporous adaptive crystals for the separation of *para*-xylene (pX) from xylene isomers. The crystal structure revealed that one host molecule can adsorb one pX molecule to form the **1**@pX complex, in which pX is located in the cavity of the host.

Xylene is an aromatic hydrocarbon in which two hydrogen atoms on the benzene ring are replaced by two methyl groups, so it has three isomers: *ortho*-xylene (***o*X**), *meta*-xylene (***m*X**), and *para*-xylene (***p*X**). Xylene isomers are important chemical feedstocks in the petrochemical and pharmaceutical industries and used for the production of many polymers, plastics, fibers, solvents, and fuel.[1–7] However, most xylenes used in industry are single-component compounds. Therefore, the prepared xylene mixtures need to be individually separated in most cases. The separation of the xylenes was classified as one of the "seven chemical separations to change the world" due to their similar kinetic sizes, close boiling points, and the same molecular weight.[8] The boiling point of ***o*X** is relatively high (417.55 K) and can be separated by rectification, while the slight difference in boiling points (only 0.8 K) between ***p*X** (411.45 K) and ***m*X** (412.25 K) makes them almost impossible to separate *via* a traditional distillation process. However, ***p*X** could be isolated by fractional crystallization due to its relatively higher melting point compared with ***m*X**.[9] However, the energy requirement for fractional crystallization is high because of the need to cool large quantities of material to about −53 °C. Therefore, it is necessary and desirable to develop easy operation and more energy efficient methods to separate ***p*X** and ***m*X**.

In the past decades, a number of methods have been developed to meet the separation challenge of xylene isomers, including solvent extraction[10–16] and adsorption by porous materials.[17–21] The method of solvent extraction sometimes has the highly toxic effect on the environment and strong corrosive effect on the equipment impeded its long term applicability. While, the adsorption by porous materials are built using reversible chemistry and have comparatively low moisture or thermal stability, which restrict their further application in industrial. Recently, macrocycle-based nonporous adaptive crystals (NACs) have attracted considerable interest as they display great potentials for practical applications, especially in the adsorption, separation, and storage of hydrocarbons.[22–31] Huang and coworkers reported the separation of ***p*X** from its structural isomers, *mX* and *oX* by nonporous adaptive crystal of pillar[6]arene with a purity of 90%.[32] Khashab's group also achieved the separation of ***p*X** using a polymorphic azobenzene cage.[33] Since the discovery of crown ethers by Pedersen in 1967, supramolecular chemistry has been developed for many years and a series of macrocyclic hosts have been designed and synthesized.[34–42] However, they have been studied as xylene isomers selective adsorbents only rarely.[43–45]

The development of NACs with high ***p*X** adsorption capacity and separation purity is still a challenging work. Herein, we report that phenanthrene[2]arene **1** can be used as a host for the encapsulation and separation of ***p*X** from the equimolar mixture of ***p*X** and ***m*X** in the vapor phases through shape selective crystallization under mild and user-friendly conditions. Furthermore, **1** exhibits excellent recyclability, with no significant decrease in performance after seven cycles of adsorption and desorption (Fig. 1).

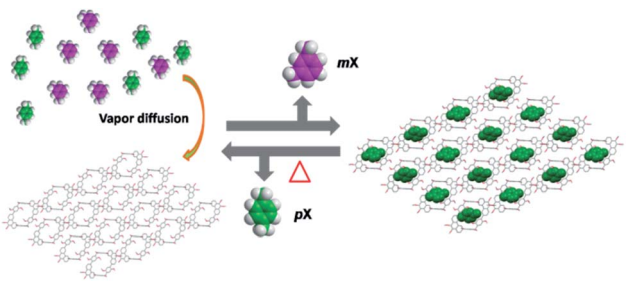

Fig. 1 Structural representation of the capture of pX from a pX/mX mixture using phenanthrene[2]arene crystals.

Department of Biology and Chemistry, Hunan University of Science and Engineering, Yongzhou 425199, China. E-mail: zengfei@iccas.ac.cn; 42979930@qq.com

† Electronic supplementary information (ESI) available: Synthesis of **2** and **3**; The ^{1}H and ^{13}C NMR spectra of **2** and **3**. CCDC 2165484 for **1**@***p*X**, 2175792 for **1**@***m*X**. For ESI and crystallographic data in CIF or other electronic format see https://doi.org/10.1039/d2ra03773d

Although, the synthesis of host **1** (ref. 46) have been reported by our group recently. However, we found that the synthetic route can be further optimized to synthesis of the precursor **3**, which is beneficial to the subsequent large-scale production. As shown in Scheme 1, starting from the commercially available 3,6-dibromophenanthrene-9,10-dione and 2,5-dimethoxyphenylboronic acid, compound **3** can be quantitatively obtained after work up by simple suction filtration by the Suzuki coupling reaction. Then, the precursor **2** can be quantitatively obtained from compound **3** through sodium dithionite reduction and methylation with dimethyl sulfate.

Similar to the phenanthrene[2]arene as the nonporous adaptive crystals for benzene adsorption capacity,[46] activated host **1** was prepared by recrystallization in the mixture of CH_2Cl_2/MeOH and dried under vacuum at 150 °C for 6 h. To study the selectivity of ***p*X** over ***m*X**, single-component solid–vapor sorption experiments were first performed with the activated solid of **1** toward ***p*X** and ***m*X**. The mole ratio of time-dependent solid–vapor sorption plots were determined by the ^{1}H-NMR analysis. As shown in Fig. 2a, the adsorption capacity of **1** toward ***p*X** in the first four hours was negligible, but the adsorption capacity of ***p*X** increased significantly with time and it required about 16 hours to reach saturation. The uptake of ***p*X** was calculated to be about one ***p*X**/**1** at saturation. Similar to the ***p*X**, activated **1** also showed adsorption capacity toward ***m*X**. However, it takes even more time for the adsorption capacity of ***m*X** to increase significantly (Fig. 2b). The uptake of ***m*X** was calculated to be about 1.2 ***m*X**/**1** at 20 hours. These results suggest that both ***p*X** and ***m*X** can be adsorb by the activated solid **1** and the absorption is a relatively slow process. Consistent with the single-component adsorption experiments, TGA analysis further confirmed the absorb number of **1** toward ***p*X** and ***m*X**. Upon heating the activated **1** that adsorbed ***p*X** or ***m*X** vapor for 20 hours, a weight loss of 9.2% from 53 to 188 °C and a weight loss of 10.8% from 48 to 145 °C were observed, which corresponded to the release of one ***p*X** molecule or 1.2 ***m*X** molecules per host **1**, respectively (Fig. 2c and d). The higher release temperature of ***p*X** than ***m*X** revealed that ***p*X** could be more steadily stored in **1** crystals than ***m*X**.

To get more information about adsorption capacity of **1** toward ***p*X** and ***m*X**, We tried to get the single crystals of **1** loaded with ***p*X** or ***m*X**. Single crystal structures that suitable for X-ray analysis were obtained by slow evaporation of the solution of **1** in ***p*X** or ***m*X**, providing unambiguous evidence for the formation of **1@*p*X** and **1@2*m*X**. As shown in Fig. 3a, the resulting crystal structure revealed that one host molecule **1** can adsorbs one ***p*X** molecule to formation of **1@*p*X** complex, in which ***p*X** located in the cavity of host. Interestingly, CH···H and CH···π interactions between ***p*X** and host **1** with the distance of 2.398 Å (a) and 2.865 Å (b) were observed. Because of these multiple noncovalent interactions, the host **1** showed high adsorption capacity for ***p*X**. Moreover, it was found that one host molecule **1** can adsorbs two ***m*X** molecules to formation of **1@2*m*X** complex (Fig. 3b), in which two ***m*X** molecules not located in the cavity of host. Additionally, CH···O and CH···π intermolecular interactions also exist between the ***m*X** and host **1**, and their distance are measured to be 2.624 Å (c) and 2.760 Å (d), respectively. From the b-axis direction of **1@*p*X** and **1@2*m*X** complex packing structure (Fig. 3c and d), a large number of ***p*X** and ***m*X** molecules are absorbed in the crystal structure. These results further support the adsorption capacity of **1** toward ***p*X**

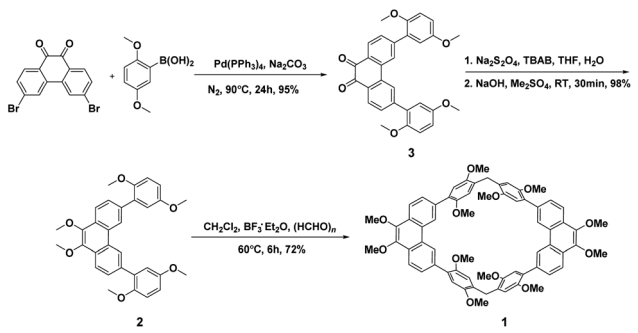

Scheme 1 Synthesis of host **1**.

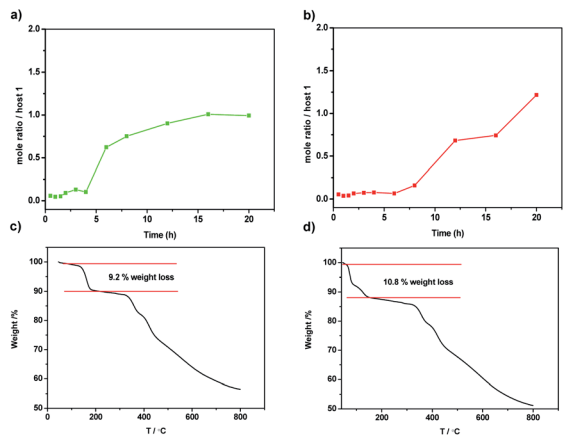

Fig. 2 (a and b) Time-dependent solid–vapor sorption plots of **1** for single-component vapour ***p*X** and ***m*X** respectively; (c and d) thermogravimetric analysis of **1** after sorption of ***p*X** or ***m*X** adsorbed vapor for 20 h.

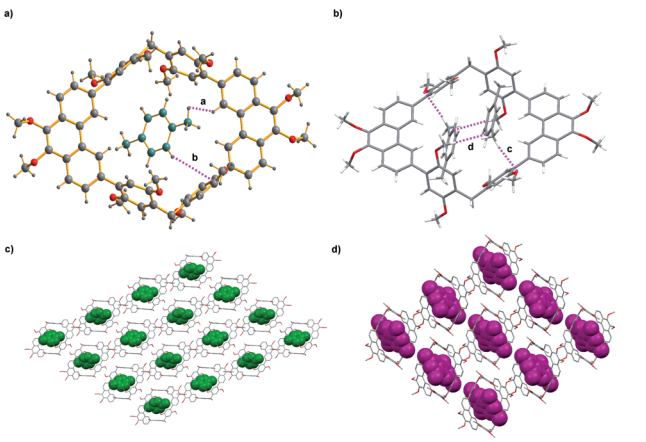

Fig. 3 Crystal structure of (a) **1@*p*X**; (b) **1@2*m*X**; (c) and (d) packing of **1@*p*X** and **1@2*m*X**, view along the *b* axis.

and ***m*X** provides us an opportunity to use host **1** as NACs material for the separation of ***p*X** and ***m*X**. Moreover, the PXRD pattern of activated solid **1** after absorbing ***p*X** showed a significant change in comparison with the original pattern of activated **1**, which suggested the structural transformation of activated **1** upon capture of ***p*X** vapour (Fig. S8†). The PXRD pattern of activated solid **1** after absorbing ***m*X** showed a no change in comparison with the original pattern of activated **1**, which suggested no structural transformation of activated **1** upon capture of ***m*X** vapour (Fig. S9†). In addition, the PXRD pattern of activated **1** after capturing ***p*X** was matched well with the simulated patterns based on single-crystal structures of **1@*p*X**. This indicated that activated **1** transformed into **1@*p*X** after adsorption of ***p*X**.

Based on the different sorption ability of activated **1** toward ***p*X** and ***m*X**, we wondered whether **1** could separate ***p*X**/***m*X** mixtures. To confirm this hypothesis, we performed two-component (1 : 1 ratio) competition sorption experiments. Similar to the single-component solid–vapor sorption experiments, the adsorption capacity of **1** toward ***p*X**/***m*X** mixtures in the first three hours was negligible. However, after 3 h, ***p*X** could be predominantly adsorbed over ***m*X** (Fig. 4a). At saturation, *ca.* 0.83 ***p*X** molecules were adsorbed with 0.18 ***m*X** molecules per activated **1** from the ^{1}H-NMR analysis (Fig. S10†). This result indicates that activated **1** has selective adsorption of ***p*X**. The Gas chromatography determined the percentage of ***p*X** adsorbed by activated **1** to be 81% (Fig. 4c). In addition the powder X-ray diffraction patterns of activated **1** that adsorbed ***p*X**/***m*X** mixtures were almost the same with the simulated patterns based on single-crystal structures of **1@*p*X** (Fig. 4b), indicating the similar ***p*X** loaded **1** crystals formed. Although, in the crystal structure of **1@2*m*X**, one host molecule can adsorbs two ***m*X** molecules, but the host **1** exhibits better ***p*X** selectivity over ***m*X**, probably due to better matching of ***p*X** in the intrinsic cavity of host **1**. Considering the further application in real production, recycling capacity is an important criterion for assessing an adsorbent. ^{1}H NMR spectroscopy and TGA analysis revealed that, by heating **1@*p*X** at 150 °C in vacuum for 3 hours, the absorbed ***p*X** could be completely released (Fig. S13 and S14†). We also proved that the newly formed crystals were activated **1** as indicated by PXRD (Fig. S15†). Moreover, the re-activated solids can be re-used in next adsorption cycles and no obviously loss of selectivity or capacity were observed after recycling seven times (Fig. 4d).

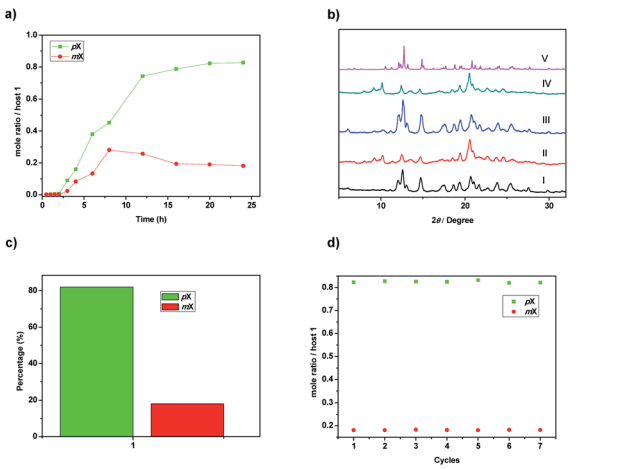

Fig. 4 (a) Time-dependent solid–vapor sorption plot of activated **1** for *p*X and *m*X equimolar mixture vapor. (b) PXRD patterns of **1**: (I) activated **1** adsorption of *p*X vapour for 20 h; (II) activated **1** adsorption of *m*X vapour for 20 h; (III) activated **1** adsorption of *p*X/*m*X mixture vapour for 20 h; (IV) activated **1** after adsorption of *p*X/*m*X mixture vapour for 20 h and then heating at 150 °C under vacuum for 3 h; (V) simulated from single-crystal structure of **1@*p*X**. (c) Relative uptakes of *p*X and *m*X adsorbed by activated **1** that adsorbed *p*X/*m*X mixtures for 20 h as measured by gas chromatography. (d) Relative uptakes of *p*X and *m*X by activated **1** that adsorbed *p*X/*m*X mixtures for 20 h after seven recycles.

Conclusions

In summary, we developed a new method for the large-scale preparation of phenanthrene[2]arene **1** and demonstrated that phenanthrene[2]arene can be used for the adsorption and separation of industrially important xylene isomers. The activated crystals of **1** showed higher ***p*X** adsorption capacity than ***m*X**. One host molecule can at maximum adsorb one ***p*X** molecules in its central cavity. Moreover, activated crystals **1** also exhibits excellent recyclability when used as NACs materials to separation of ***p*X** and ***m*X**. The advantages of simple synthesis, high separation efficiency, and outstanding recycling performance of **1** makes this material possesses enormous potential for applications in the chemical industry.

Conflicts of interest

There are no conflicts to declare.

Acknowledgements

We are grateful for the financial support from the National Natural Science Foundation of China No. 21602055 and 51772091; Natural Science Foundation of Hunan Province No. 2017JJ3094.

Notes and references

1 Y. Yang, P. Bai and X. Guo, *Ind. Eng. Chem. Res.*, 2017, **56**, 14725–14753.
2 M. I. Gonzalez, M. T. Kapelewski, E. D. Bloch, P. J. Milner, D. A. Reed, M. R. Hudson, J. A. Mason, G. Barin, C. M. Brown and J. R. Long, *J. Am. Chem. Soc.*, 2018, **140**, 3412–3422.
3 W. J. Cannella, *Xylenes and ethylbenzene*, Wiley and Sons, New York, 2000.
4 R. Meyers, *Handbook of Petroleum Refining Processes*, 3th ed., McGraw-Hill, New York, 2003, pp. 2.47–2.53.
5 J. Scheirs and T. E. Long, *Industrial Modern Polyesters: chemistry and technology of polyesters and copolyesters*, Wiley, Chichester, 2003.

6 J. L. Pellegrino, *Energy and Environmental Profile of the Chemicals Industry*, U.S. Department of Energy, 2000.
7 N. Sun, S.-Q. Wang, R. Zou, W. G. Cui, A. Zhang, T. Zhang, Q. Li, Z. Z. Zhuang, Y. H. Zhang, J. Xu, M. J. Zaworotko and X. H. Bu, *Chem. Sci.*, 2019, **10**, 8850–8854.
8 D. S. Sholl and R. P. Lively, *Nature*, 2016, **532**, 435–437.
9 D. Ruthven, *Principles of Adsorption and Adsorption Processes*, Wiley, New York, 1984, pp. 401–405.
10 D. A. McCaulay, B. H. Shoemaker and A. P. Lien, *Ind. Eng. Chem.*, 1950, **42**, 2103–2107.
11 G. Zhang, A.-H. Emwas, U. F. S. Hameed, S. T. Arold, P. Yang, A. Chen, J.-F. Xiang and N. M. Khashab, *Chem*, 2020, **6**, 1082–1096.
12 F. U. Rahman, J.-M. Yang, Y.-H. Wan, H.-B. Zhang, I. D. Petsalakis, G. Theodorakopoulos, J. Rebek and Y. Yu, *Chem. Commun.*, 2020, **56**, 6945–6948.
13 G. Zhang, B. Moosa, A. Chen and N. M. Khashab, *ChemPlusChem*, 2020, **85**, 1244–1248.
14 I. Uemasu, *J. Inclusion Phenom. Mol. Recognit. Chem.*, 1992, **13**, 1–7.
15 I. Uemasu and S. Kushiyama, *Fuel Process. Technol.*, 2004, **85**, 1519–1526.
16 H. F. Yang and Y. F. Hu, *Chem. Eng. Process.*, 2017, **116**, 114–120.
17 D. M. Polyukhov, A. S. Poryvaev, S. A. Gromilov and M. V. Fedin, *Nano Lett.*, 2019, **19**, 6506–6510.
18 M. du Plessis, V. I. Nikolayenko and L. J. Barbour, *J. Am. Chem. Soc.*, 2020, **142**, 4529–4533.
19 M. B. Dewal, M. W. Lufaso, A. D. Hughes, S. A. Samuel, P. Pellechia and L. S. Shimizu, *Chem. Mater.*, 2006, **18**, 4855–4864.
20 W. Huang, J. Jiang, D. Wu, J. Xu, B. Xue and A. M. Kirillov, *Inorg. Chem.*, 2015, **54**, 10524–10526.
21 T. Ogoshi, Y. Shimada, Y. Sakata, S. Akine and T. Yamagishi, *J. Am. Chem. Soc.*, 2017, **139**, 5664–5667.
22 J. R. Wu and Y. W. Yang, *J. Am. Chem. Soc.*, 2019, **141**, 12280–12287.
23 Y. Zhou, K. Jie, E. Li and F. Huang, *Sci. Sin.: Chim.*, 2019, **49**, 832–843.
24 M. Wang, J. Zhou, E. Li, Y. Zhou, R. Zhao, W. Zhu and F. Huang, *J. Am. Chem. Soc.*, 2019, **141**, 17102–17106.
25 K. Jie, Y. Zhou, E. Li, R. Zhao, M. Liu and F. Huang, *J. Am. Chem. Soc.*, 2018, **140**, 3190–3193.
26 Y. Ding, L. O. Alimi, B. Moosa, C. Maaliki, J. Jacquemin, F. Huang and N. M. Khashab, *Chem. Sci.*, 2021, **12**, 5315–5318.
27 H. Yao, Y.-M. Wang, M. Quan, M. U. Farooq, L.-P. Yang and W. Jiang, *Angew. Chem., Int. Ed.*, 2020, **59**, 19945–19950.
28 Y. Zhao, H. Xiao, C.-H. Tung, L.-Z. Wu and H. Cong, *Chem. Sci.*, 2021, **12**, 15528–15532.
29 J. R. Wu and Y.-W. Yang, *Angew. Chem., Int. Ed.*, 2021, **60**, 1690–1701.
30 W. Yang, K. Samanta, X. Wan, T. U. Thikekar, Y. Chao, S. Li, K. Du, J. Xu, Y. Gao, H. Zuilhof and A. C. Sue, *Angew. Chem., Int. Ed.*, 2020, **59**, 3994–3999.
31 K. Jie, Y. Zhou, E. Li and F. Huang, *Acc. Chem. Res.*, 2018, **51**, 2064–2072.
32 K. Jie, M. Liu, Y. Zhou, M. A. Little, A. Pulido, S. Y. Chong, A. Stephenson, A. R. Hughes, F. Sakakibara, T. Ogoshi, F. Blanc, G. M. Day, F. Huang and A. I. Cooper, *J. Am. Chem. Soc.*, 2018, **140**, 6921–6930.
33 B. Moosa, L. O. Alimi, A. Shkurenko, A. Fakim, P. M. Bhatt, G. Zhang, M. Eddaoudi and N. M. Khashab, *Angew. Chem., Int. Ed.*, 2020, **59**, 21367–21372.
34 C.-F. Chen, *Chem. Commun.*, 2011, **47**, 1674–1688.
35 M.-X. Wang, *Acc. Chem. Res.*, 2012, **45**, 182–195.
36 T. Ogoshi, S. Kanai, S. Fujinami, T.-A. Yamagishi and Y. Nakamoto, *J. Am. Chem. Soc.*, 2008, **130**, 5022–5023.
37 X.-N. Han, Y. Han and C.-F. Chen, *J. Am. Chem. Soc.*, 2020, **142**, 8262–8269.
38 H. Chen, J. Fan, X. Hu, J. Ma, S. Wang, J. Li, Y. Yu, X. Jia and C. Li, *Chem. Sci.*, 2015, **6**, 197–202.
39 M.-H. Ding, J. Liao, L.-L. Tang and F. Zeng, *Chin. Chem. Lett.*, 2021, **32**, 1665–1668.
40 Q.-H. Guo, L. Zhao and M.-X. Wang, *Angew. Chem., Int. Ed.*, 2015, **54**, 8386–8389.
41 Q. Shi, X. Wang, B. Liu, P. Qiao, J. Li and L. Wang, *Chem. Commun.*, 2021, **57**, 12379–12405.
42 F. Zeng, L. Cheng, G. C. Ou, L.-L. Tang and M. H. Ding, *J. Org. Chem.*, 2022, **87**, 3863–3867.
43 G. Zhang, B. Hua, A. Dey, M. Chosh, B. A. Moosa and N. M. Khashab, *Acc. Chem. Res.*, 2021, **54**, 155–168.
44 A. Dey, S. Chand, M. Ghosh, M. Altamimy, B. Maity, P. M. Bhatt, I. A. Bhat, L. Cavallo, M. Eddaoudi and N. M. Khashab, *Chem. Commun.*, 2021, **57**, 9124–9127.
45 G. Zhang, Y. Ding, A. Hashem, A. Fakim and N. M. Khashab, *Cell Rep. Phys. Sci.*, 2021, **2**, 100470.
46 F. Zeng, L. Cheng, L.-L. Tang and X. F. Wang, *Org. Chem. Front.*, 2022, **9**, 3307–3311.